JOURNAL OF APPLIED ELECTROCHEMISTRY **28** (1998) 251–258

Evaluation of carbon electrodes and electrosynthesis of coumestan and catecholamine derivatives in the FM01-LC electrolyser*

D. SZÁNTO, P. TRINIDAD‡, F. WALSH§

Applied Electrochemistry Group, School of Pharmacy, Biomedical and Physical Sciences, University of Portsmouth, St Michael's Building, White Swan Road, Portsmouth, PO1 2DT, Great Britain

Received 9 April 1997; revised 21 July 1997

This work extends the range of electrodes and conditions under which the FM01-LC reactor has been used in a laboratory environment and evaluates the performance of carbon electrodes. Reticulated vitreous carbon (RVC) has been used to provide a stable, inert, three-dimensional electrode surface for organic electrosynthesis; its performance is compared to that of nickel mesh for the oxidation of catechol to *o*-quinone. This product was then reacted *in situ* with (i) 4-hydroxycoumarin and (ii) 1,3-dimethylbarbituric acid to produce, respectively, coumestan and catecholamine, products of synthetic interest. In mass transport experiments using hydroquinone oxidation as a model reaction, performance was similar to nickel electrodes, but Sherwood numbers were reduced by about 5–10% when carbon electrodes were used. The best-performing RVC electrode, however, showed poorer behaviour than its nickel counterpart. Yields for the production of coumestan and catecholamine were approximately 45% and 25%, respectively, although this was mostly due to extraction problems, since current efficiencies were both in the region of 65–70%. The electrode material, rather than the fluid flow behaviour, leads to a reduction in overall cell efficiency; this is confirmed by studies which show a film forming on the surface of the electrode.

Keywords: *filter press*, *parallel plate*, *electrochemical reactor design*, *electroorganic synthesis*, *FM01-LC electrolyser*

List of symbols

A projected electrode area (m^2)
A_e electrode area per unit volume of electrode ($m^2\,m^{-3}$)
B depth of the electrolyte channel (m)
c concentration of electroactive species ($mol\,m^{-3}$)
c_B concentration of electroactive species in the bulk electrolyte ($mol\,m^{-3}$)
D diffusion coefficient of reactant species ($m^2\,s^{-1}$)
F Faraday constant ($C\,mol^{-1}$)
k_m averaged mass transfer coefficient ($m\,s^{-1}$)
I_L limiting current (due to convective diffusion of reactant) (A)
L characteristic length (hydraulic diameter of flow channel) (m)
Re Reynolds number ($Re = vL/v$)
S width of the electrolyte channel (m)
Sc Schmidt number ($Sh = v/D$)
Sh Sherwood number ($Sh = k_mL/D$)
t time (s)
v mean linear flow velocity ($m\,s^{-1}$)
X_A fractional conversion of reactant
z number of electrons per reactant molecule

Greek symbols
η overpotential (V)
v kinematic viscosity of the electrolyte ($m^2\,s^{-1}$)

1. Introduction

The parallel plate, filter-press, reactor is the most common type of electrolyser for both laboratory and industrial applications. Filter press cells have found application in both inorganic and organic synthesis, as fuel cells and redox batteries, and in environmental treatment processes [1]. A number of 'off-the-shelf' reactors are now available, which have been well characterized in the literature [2]. Further work is needed to establish suitable applications for these reactors, particularly in the area of electrosynthesis where, historically, electrochemical technology has lagged behind conventional chemical techniques [3].

* The paper was presented at the Fourth European Symposium on Electrochemical Engineering, Prague, 28–30 August 1996.
‡ Now at: Tecnicas Reunidas, S.A., Centro de Investigación C/Sierra Nevada, 16 PO Ind. San Fernado II, 28850 Torrejon de Ardoz, Madrid, Spain.
§ Author for correspondence.

0021-891X

Conversely, it is often necessary to build filter press cells for a specific task, in which case full characterization is necessary in terms of appropriate figures of merit [4] such as the averaged mass transfer rates, pressure drops and flow distribution.

The FM01-LC electrolyser uses a conventional monopolar filter press design with a projected electrode surface area of 64 cm^2. It was designed as a scale model of the FM21-SP electrolyser, used in the chlor-alkali industry, which has an electrode area of 21 dm^2 [1]. The FM01-LC has previously been characterized in terms of global [5] and local [6] mass transport to electrodes, the performance of three-dimensional electrodes [7], pressure drop over electrolyte channels [8] and hydrodynamic behaviour using a simple moment analysis [9]. The use of carbon electrodes for organic synthesis has been known for some time, and reticulated vitreous carbon (RVC) has shown promise due to its large surface area per unit volume [10]. RVC electrodes have been studied for copper deposition both as rotating cylinders [11] and in filter press cells [12]. This work further characterizes the FM01-LC electrolyser by studying mass transport and conversion rates during electrochemical oxidations at carbon electrodes and investigates the use of RVC electrodes of differing pore sizes.

2. Experimental details

The FM01-LC electrolyser (Fig. 1) used two nickel or graphite flat-plate electrodes constructed from a single sheet of graphite (e) (LeCarbone) separated by PTFE spacers (s) which also acted as flow-dispersers. The projected electrode area was 16 cm × 4 cm. Hydraulic sealing was established by PTFE gaskets. The entire assembly was then held in place by two end-plates. The global mass transport was increased, as required, by the addition of turbulence promoters placed between the two electrodes in the flow path. The characteristics and dimensions of both (Netlon™) turbulence promoters are given in Table 1. In all experiments, a cation-exchange membrane, Nafion® 324 (DuPont), was used to separate the anolyte and catholyte compartments. All experiments were performed at 295 K.

The hydraulic circuit (Fig. 1) consisted of two glass reservoirs (5 dm^3) containing the anolyte (a) and catholyte (b), respectively. Two pumps (c) (Totton Pumps) were used to circulate the electrolytes at flow

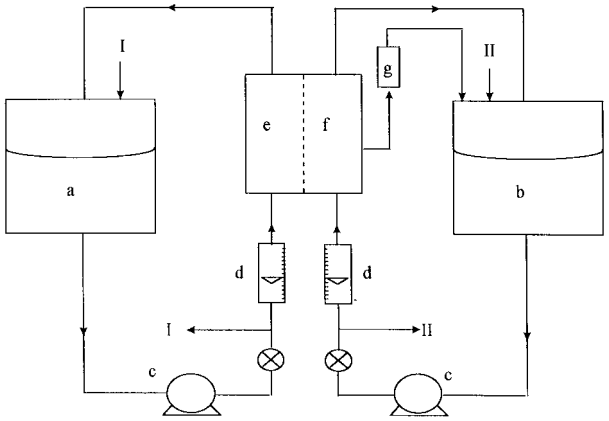

Fig. 1. Hydraulic circuit used for mass transport measurements and electrosynthesis in the FM01-LC electrolyser. Key: (a) anolyte reservoir, (b) catholyte reservoir, (c) pump, (d) rotameter, (e) anolyte compartment, (f) catholyte compartment, (g) reference electrode compartment.

rates of 1–10 $cm^3\ s^{-1}$. The flow was then passed through the electrolyser (d) and back into the reservoir. Bypasses were included (points I and II) to enable the flow rate to be altered while running the pumps at full power). A PTFE capillary tube (i.d. 1 mm) was inserted into the anodic spacer to allow electrolyte to slowly flow into a reference electrode compartment (g), containing a saturated calomel electrode (SCE); electrolyte was recycled to the reservoir.

Mass transport measurements were made using the well-known limiting diffusion current technique [13]. The oxidation of hydroquinone (Fisons, 0.001 mol dm^{-3} in a 0.5 mol dm^{-3} mixed phosphate buffer at pH 7) was used to measure limiting currents. The averaged mass transfer coefficient, k_m, was then calculated from

$$k_m = \frac{I_L}{zFAc_B} \tag{1}$$

where k_m is the averaged mass transfer coefficient, I_L the limiting current, z the number of electrons per reactant molecule, F the Faraday constant (96 485 C mol^{-1}), A the active electrode surface area (taken as the projected area of 64 cm^2) and c_B the bulk concentration of reactant in the electrolyte.

Two electrochemical syntheses were performed, involving reaction of the oxidation product of catechol in the presence of either (i) 4-hydroxycoumarin or (ii) 1,3-dimethylbarbituric acid. In each case,

Table 1. Characteristics of the two turbulence promoters used [7]

*Promoter**	*Material*	*CD*† /mm	*LD*‡ /mm	*Orientation in direction of flow*	*Overall voidage*§
'Greenhouse Shading' (A)	Blown polyethylene	7	7	N/A	0.80
CE121 (B)	PTFE	7	28	CD	0.84

* Both promoters were cut to 16 cm × 4 cm to correspond to the projected electrode area.
† CD is the internal dimension across shorter diagonal.
‡ LD is the internal dimension across longer diagonal.
§ Overall voidage is the ratio of free space in the channel to overall channel volume.

nickel and carbon electrodes were considered. In all experiments, the background electrolyte was sodium acetate ($0.15\,mol\,dm^{-3}$ in doubly-distilled water) which has a pH 9 and thus prevents the reformation of catechol from the oxidation product. Quantitative measurements were made by determining the drop in catechol concentration via GC (Hewlett Packard 5890 SRS II) using a fused silica bonded phase capillary column (30 m, i.d. 0.25 mm). Preparative electrolyses were terminated after an electrical charge corresponding to $2\,F\,mol^{-1}$ of the reactant had been passed. The electrolyte was then discharged from the reservoir, glacial acetic acid (7 aliquots, each of $0.1\,cm^3$) was added, dropwise, and the mixture was placed in a refrigerator (at $\simeq 5$ °C) until crystallization occurred, taking between two and four days. The product was filtered under vacuum and washed with four, successive $5\,cm^3$ aliquots of acetone. The solid was filtered and dried in a desiccator (24 h) before weighing.

3. Results and discussion

3.1. *Mass transport measurements*

In contrast to previous work published on the FM01-LC electrolyser, which utilized a variety of copper, nickel or stainless steel electrode materials [5–8], the mass transport performance of various carbon electrodes has been studied here. When using the limiting diffusion current technique, it is common to choose a model reaction such as copper deposition or oxidation of ferricyanide ion [14]. However, studies have shown that neither of these reaction systems are well-suited to carbon electrodes [15] and the oxidation of hydroquinone in phosphate buffer was used. This has three advantages: (i) since the process is anodic, there is no need to degas the solution to prevent oxygen reduction, (ii) the surface area of the carbon is unaffected by, for example, metal deposition on the surface, and (iii) the quinone/hydroquinone system can act as a model reaction for certain organic and biochemical reactions. The quinone/hydroquinone electrolyte solution does, however, degrade with time (by photooxidation of the hydroquinone to quinone) and must be freshly prepared daily.

Polarization curves for the oxidation of hydroquinone were recorded at various flow rates for each configuration of reactor studied. Figure 2 shows curves recorded at flat-plate carbon electrodes in the absence of a turbulence promoter. The limiting current plateaux are well-defined, flat, and long (taking place over an approximate potential range of 600 mV).

Values for the limiting current, and hence the mass transfer coefficient, k_m, were measured at carbon electrodes using both the Netlon™ 'Greenhouse Shading' turbulence promoter and the Netlon™ CE121 turbulence promoter. These data are plotted as dimensionless group correlations of Sherwood number, *Sh*, against Reynolds number, *Re*. The Sherwood number represents the mass transport in the system and is given by

$$Sh = \frac{k_m L}{D} \tag{2}$$

where L is a representative length for the reactor and D is the diffusion coefficient of reactant species in the electrolyte. For the FM01-LC reactor, L can be taken as the hydraulic diameter of flow channel:

$$L = \frac{2BS}{B+S} \tag{3}$$

where S is the width of the electrolyte channel and B is the (compressed) depth of the electrolyte channel. The Reynolds number is given by

$$Re = \frac{vL}{v} \tag{4}$$

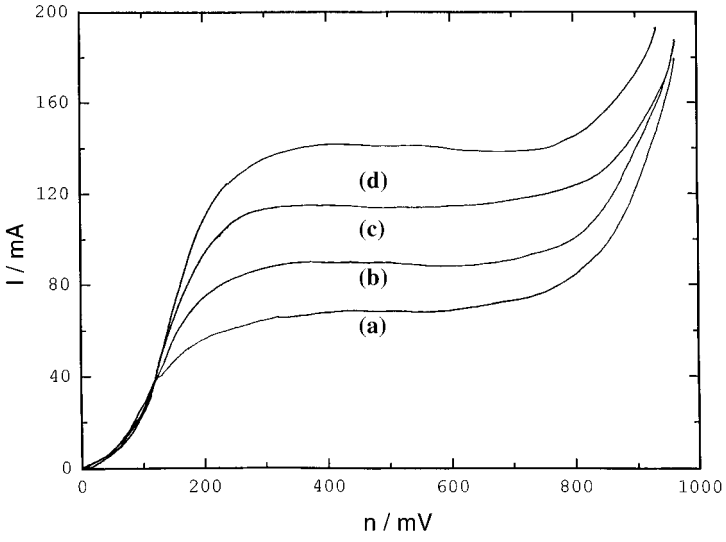

Fig. 2. Current against potential curves illustrating the effect of mean linear flow velocity variation on the limiting current for the oxidation of hydroquinone ($10\,mmol\,dm^{-3}$ in phosphate buffer) at carbon electrodes in the FM01-LC electrolyser. Velocity: (a) 10, (b) 15, (c) 20 and (d) $25\,cm\,s^{-1}$.

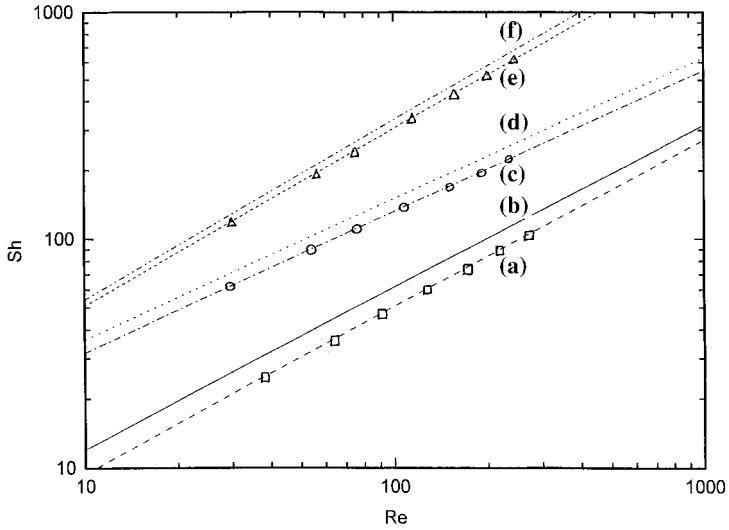

Fig. 3. Log-log plots of Sherwood numbers against Reynolds number comparing the performance of carbon and nickel electrodes with turbulence promoters. Electrodes: (a) carbon flat plate, (b) nickel flat plate (from [6]), (c) carbon flat plate with turbulence promoter A, (d) nickel flat plate with turbulence promoter A (from [6]), (e) carbon flat plate with turbulence promoter B, (f) nickel flat plate with turbulence promoter B (from [6]).

where v is the mean linear electrolyte velocity and ν is the kinematic viscosity of the electrolyte. The Sh against Re correlations can be used to compare different configurations in different reactors. By plotting the data of Sh against Re, the performance of a reactor can be described by

$$Sh = a\,Re^{b}\,Sc^{c} \tag{5}$$

The Schmidt number, Sc, represents the transport properties of the electrolyte and is given by

$$Sc = \frac{\nu}{D} \tag{6}$$

The performance of the carbon electrodes can be seen in Fig. 3. The data are compared to the values recorded using nickel electrodes. The mass transport to carbon electrodes is apparently slightly lower than that to nickel electrodes. The same mass transport enhancement can be seen for the turbulence promoters as seen in the previous study [7]. It must be stressed that in no way can the electrode *material* affect the rate of mass transport. The correlations fitted to the data are given in Table 2.

The performance of reticulated vitreous carbon electrodes was also studied in the FM01-LCl cell. In this case, the exact electrode surface area is not known, and the correlation used is of the form:

$$k_{\mathrm{m}}A_{\mathrm{e}} = \alpha v^{\beta} \tag{7}$$

where A_{e} is the electrode area per unit volume of electrode for the RVC. Three grades of RVC were studied, having 100, 60 and 30 ppi (nominal pores per linear inch). The performance of these was compared to that of three-dimensional nickel electrodes in the FM01-LC (Fig. 4). The performance of wide-pore RVC (60 and 30 ppi) can be seen to be relatively poor. Whilst these two grades of RVC have been used in the form of rotating cylinders [11], results from two separate studies [12, 16] have established that small-pore (high ppi grade number) RVC electrodes have a greater value of active electrode area per unit electrode volume than wide-pore ones. The 100 ppi RVC has a performance roughly comparable to that of a nickel mesh, according to [7]. If the 5–10% reduction in current due to conductivity as described above is taken into account, the performance of RVC is approximately the same as that of the nickel stacked net. Although no results for nickel foam are presented here, extrapolation from other studies in parallel plate cells [17] would imply a further significant enhancement. The correlation equations for these three-dimensional electrodes are summarized in Table 3.

Table 2. Dimensionless group correlations of the form $Sh = a\,Re^{b}\,Sc^{c}$ for various configurations of the FM01-LC electrolyser

Correlation in Fig. 4	*Configuration*	*a*	*b*	*c*
(a)	Carbon flat plate	0.15	0.73	0.33
(b)	Nickel flat plate	0.22	0.71	0.33
(c)	Carbon flat plate + turbulence promoter A	0.65	0.62	0.33
(d)	Nickel flat plate + turbulence promoter A	0.74	0.62	0.33
(e)	Carbon flat plate + turbulence promoter B	0.72	0.78	0.33
(f)	Nickel flat plate + turbulence promoter B	0.75	0.79	0.33

Note: Correlation coefficients exceeded 0.99 in all cases; $C = 0.33$ is assumed.

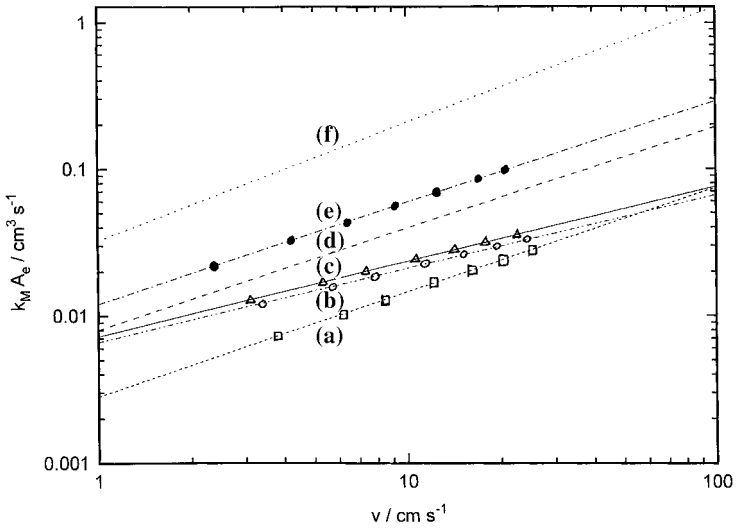

Fig. 4. Log-log plots of $k_m A_e$ against v comparing the performance of various three-dimensional electrodes. Key: (a) carbon flat plate, (b) RVC 30 ppi, (c) RVC 60 ppi, (d) nickel mesh (Twin Grid TWB from [7]), (e) RVC 100 ppi, (f) nickel stacked net (from [7]). Limiting currents at nickel electrodes measured from ferricyanide reduction (1 mmol dm^{-3} in 0.5 mol dm^{-3} KOH), those at carbon electrodes measured from hydroquinone oxidation (10 mmol dm^{-3} in phosphate buffer).

3.2. *Organic electrosynthesis*

The use of three-dimensional electrodes for the synthesis of organic compounds in the FM01-LC electrolyser has been described for the oxidation of alcohols. In the case of the oxidation of isopropylidene glycerol [7], low product yields of 21% were obtained at nickel electrodes but the *selectivity* of the process was very high, with no other products being found. Therefore, it was decided to study a reaction to illustrate: (i) the difference in performance between carbon and nickel electrodes and (ii) a further example of a successful electrosynthesis on a scaleable laboratory scale.

The oxidation of catechol at both nickel hydroxide and carbon electrodes is well known [18] according to the scheme shown in Fig. 5. The cyclic voltammogram of catechol (Fig. 5A) shows a clear oxidation peak at +0.25 V vs SCE, to the unstable *o*-quinone product (Fig. 5B). In the presence of a nucleophile (Fig. 5C or 5F), a Michael-type addition occurs to produce the related heterocyclic compound (Fig. 5E or 5G). The coumestan product is one of a group of compounds which have a structure relevant to several natural products of physiological interest [19].

Table 3. Correlations of the form $k_m A_e = \alpha v^{\beta}$ for various configurations in FM01 LC electrolyser

Correlation in Fig. 4	*Configuration*	$10^2 \times \alpha$/cm s^{-1}	β
(a)	Carbon flat plate	0.28	0.71
(b)	RVC 30 ppi	0.66	0.50
(c)	RVC 60 ppi	0.72	0.51
(d)	Nickel TWB	0.80	0.69
(e)	RVC 100 ppi	1.20	0.69
(f)	Nickel mesh	3.20	0.80

Note: Correlation coefficients exceeded 0.99 in all cases.

The current–potential curves for the oxidation of catechol in sodium acetate at various flow rates were measured for the flat-plate graphite electrode (Fig. 6, inset). The presence of a well-defined set of limiting current plateaux confirms that the reaction is, initially at least, occurring at clean electrodes. In the absence of a nucleophile (and as an inefficiency in the normal electrolysis), the *o*-quinone is unstable and forms a polymeric passivating film. Therefore, to quantitatively assess the conversion efficiency of the configu-

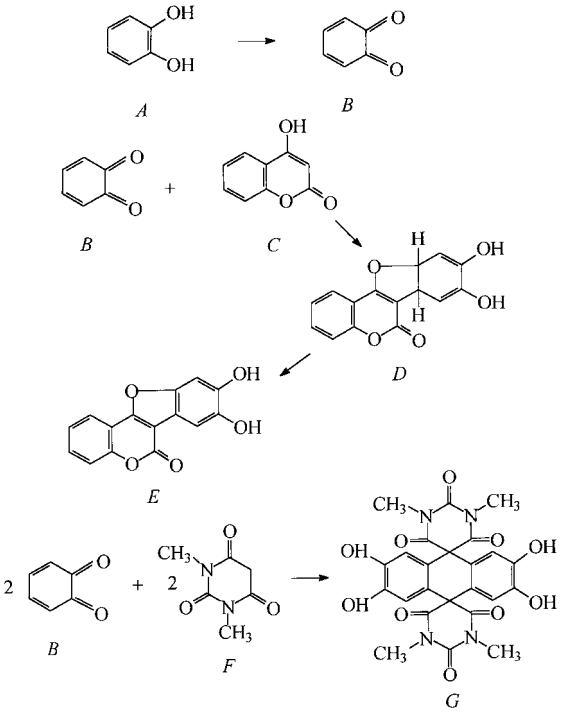

Fig. 5. Reaction scheme describing electrooxidations performed. (A) catechol; (B) orthoquinone; (C) 2-hydroxycoumarin; (D) 1,6-dihydrocoumestan; (E) coumestan; (F) *N*,*N*-dimethylbarbituric acid; (G) bis spiro(5,5′)-2,4,6-trioxo-pyrimidinyl[5,5′:10,10′] anthracene.

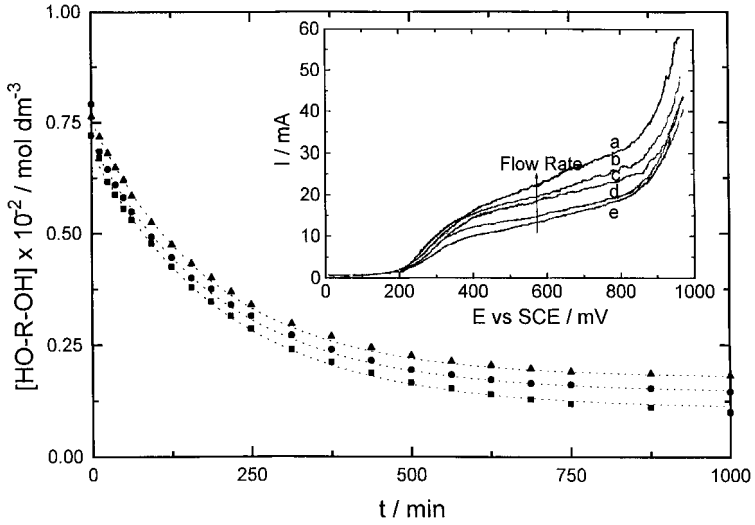

Fig. 6. Plots of concentration against time comparing the effect of differing flow rates: (▲) 15, (●) 20 and (■) 25 cm s^{-1}. Inset: plots of current against potential comparing the effect of flow velocities: (a) 10, (b) 15, (c) 20, (d) 25 and (e) 30 cm s^{-1}. Linear potential sweep rate 1 mV s^{-1}.

rations studied, the rate of loss of catechol in sodium acetate was measured with the inclusion of an excess of 4-hydroxycoumarin at a constant potential of 1.00 V vs SCE. This was performed for a series of flow rates (Fig. 6). A typical exponential decay was seen, with current efficiencies in the region of 80% for the oxidation of catechol. These data are also presented as fractional conversion against time for a variety of flow rates (Fig. 7). Since the reaction control is potentiostatic, the reaction follows first-order kinetics at all times [20].

The performance of the reactor can be established by calculating the time taken for a fractional conversion of 90%. These data are shown plotted against Reynolds number for the six configurations studied (Fig. 8). It can be seen that, in terms of catechol consumption, the reactor is highly efficient and that the more conductive surface of the nickel appears to give rise to a more rapid conversion when compared to carbon. The rate of mass transport can be established by measuring the reaction rate from the concentration against time curves. From these results (summarized in Table 4), we can see that the *apparent* mass transfer is significantly reduced by about 20%. This is attributed to formation of some polymeric film on the electrode surface. Again, these values are not intended to be an accurate description of the mass transport in the reactor, rather they are an indication of the expected performance under these reaction conditions.

The preparative electrolyses of catechol in the presence of (i) 4-hydroxycoumarin and (ii) 1,3-dimethylbarbituric acid were carried out in the FM01-LC at constant potentials of 1.20 V and 0.80 V, respectively, using published methods [21, 22]. In both cases, the products were confirmed by NMR spectroscopy as compounds E and G in Fig. 5. The current efficiencies for the process, based on coulometric

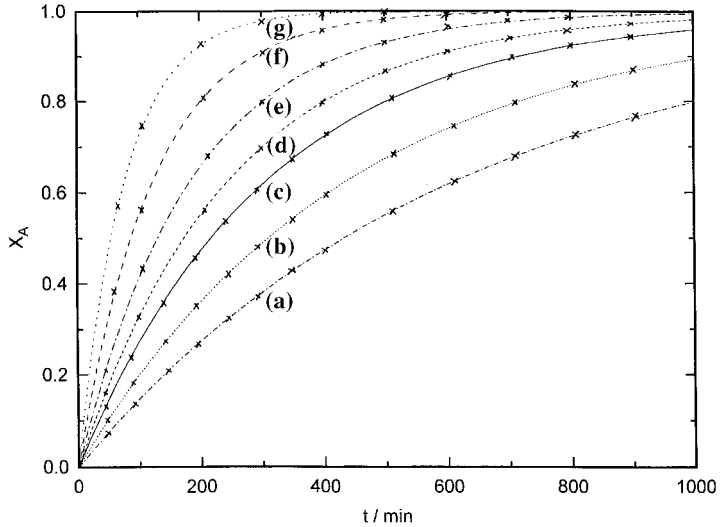

Fig. 7. Plots of fractional conversion of catechol against time showing the effect of various mean linear flow velocities: (a) 2, (b) 5, (c) 10, (d) 15, (e) 20, (f) 25 and (g) 30 cm s^{-1}.

Table 4. Comparison between mass transport correlations measured by the limiting diffusion-current technique and apparent values measured during electrooxidation of catechol

Configuration	*Mass transport correlation as measured using LCDT**	*Mass transport correlation measured during synthesis*†	*Percentage decrease in apparent mass transport*‡
Flat plate nickel	$Sh = 0.22\,Re^{0.71}\,Sc^{0.33}$	$Sh = 0.17\,Re^{0.72}\,Sc^{0.33}$	23
Flat plate carbon	$Sh = 0.15\,Re^{0.73}\,Sc^{0.33}$	$Sh = 0.12\,Re^{0.72}\,Sc^{0.33}$	22
Flat plate nickel + turbulence promoter A	$Sh = 0.74\,Re^{0.62}\,Sc^{0.33}$	$Sh = 0.61\,Re^{0.62}\,Sc^{0.33}$	18
Flat plate carbon + turbulence promoter A	$Sh = 0.65\,Re^{0.62}\,Sc^{0.33}$	$Sh = 0.51\,Re^{0.63}\,Sc^{0.33}$	21
RVC 60 ppi	$k_mA_e = 0.72 \times 10^{-2}\,v^{0.51}$	$k_mA_e = 0.59 \times 10^{-2}\,v^{0.50}$	18
RVC 100 ppi	$k_mA_e = 1.20 \times 10^{-2}\,v^{0.69}$	$k_mA_e = 0.90 \times 10^{-2}\,v^{0.69}$	25
Nickel mesh	$k_mA_e = 3.20 \times 10^{-2}\,v^{0.80}$	$k_mA_e = 2.56 \times 10^{-2}\,v^{0.78}$	20

* From ferricyanide ion reduction (1 mmol dm^{-3} in 0.5 mol dm^{-3} KOH) in the case of nickel electrodes and hydroquinone oxidation (10 mmol dm^{-3} in phosphate buffer at pH 7) in the case of carbon electrodes.

† From rate constants calculated from the decay of concentration during oxidation of catechol at various mean linear flow velocities in the range 5–30 cm s^{-1}.

‡ The decrease is stated as the value obtained from electrosynthesis measurements, in comparison to the value measured by the limiting current diffusion technique. The mean of 10 determinations of each has been used in the comparison.

measurements, were (i) 66% and (ii) 75%, based on rate of catechol consumption. The achieved yields of product were (i) 45% and (ii) 25% based on amount of pure product. No impurities were found, and the selectivity of the process was high. Ultimately, the cause of the low yields is the formation of a film on the surface of the electrode, which appears as a solid, green smear. It has been suggested that this is a dimeric product of catechol [21]; mass spectroscopic measurements indicated catechol fragments, which is consistent with either a mono- or polymeric product of catechol. In a batch reactor, this film can be removed simply with acetone but this is impossible in a (continuous flow-through) filter-press cell. It is hoped that further studies can establish an electrochemical, *in situ* method for removal of this film.

4. Conclusions

The performance of carbon electrodes in the FM01-LC laboratory electrolyser is comparable to that of nickel electrodes previously characterized, but limiting currents measured are approximately 5–10% lower. This is attributable to a reduced activity of carbon compared to nickel and it is hoped that further studies could evaluate more active carbon surfaces to alleviate this effect. When oxidizing catechol in the FM01-LC, a polymeric film on the surface of the electrode slowly reduces the limiting currents by a further 10–15% and proved difficult to remove. Preparative electroorganic syntheses of coumestan and catecholamine products proved successful, at low yields but with high selectivity. Fluid flow measurements of the various configurations used in this study, including RVC [23], show that there is no significant by-pass occurring in the reactor, and therefore the reduced efficiency at these conditions is solely due to surface electrochemical effects. Further studies will aim to elucidate the structure of this polymeric film and its quantitative effect on the electrosynthesis.

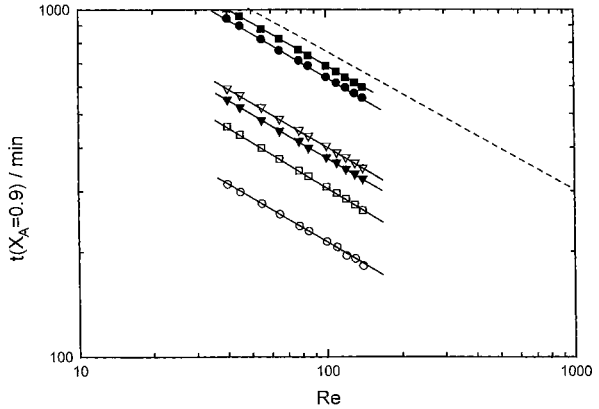

Fig. 8. Plots showing the relationship between Reynolds number and the time taken to achieve a 0.90 fractional conversion of catechol reactant for various configurations of the FM01-LC used in this study. Key: (■) flat plate nickel, (●) flat plate carbon, (▼) flat plate nickel with turbulence promoter, (▽) flat plate carbon with turbulence promoter, (□) 100 ppi RVC, (○) nickel mesh, (- - - - -) values predicted from mass transport data.

Acknowledgements

The authors are grateful to David Rees who carried out some preliminary studies on organic electrosynthesis. Financial support for the studies has been provided by a European Union grant (to Pedro Trinidad) and an EPSRC studentship (to Dominic Szánto).

References

[1] F. C. Walsh and D. Robinson, *Chemical Technology Europe*, May/June, (1995) 16.
[2] D. Pletcher and F. C. Walsh, 'Industrial Electrochemistry', 2nd edn, Chapman & Hall, London (1990), p. 146.
[3] P. M. Bersier, L. Carlsson and J. Bersier, Electrochemistry for a Better Environment, in 'Topics in Current Chemistry', Springer-Verlag, Berlin (1994), p. 113.
[4] F. C. Walsh, 'A First Course in Electrochemical Engineering', The Electrochemical Consultancy, Romsey, UK (1993), p. 199
[5] C. J. Brown, D. Pletcher, F. C. Walsh, J. K. Hammond and D. Robinson, *J. Appl. Electrochem.* **23** (1993) 38.

[6] C. J. Brown, D. Pletcher, F. C. Walsh, J. K. Hammond and D. Robinson, *ibid.* **22** (1992) 613.
[7] C. J. Brown, D. Pletcher, F. C. Walsh, J. K. Hammond and D. Robinson, *ibid.* **24** (1994) 95.
[8] C. J. Brown, F. C. Walsh and D. Pletcher, *Trans. I. Chem. E.* **73**(A) (1995) 196.
[9] P. Trinidad and F. C. Walsh, *Electrochim. Acta* **41** (1996) 493.
[10] J. H. Wang, *ibid.* **26**, (1981) 1721.
[11] A. H. Nahlé, G. W. Reade and F. C. Walsh, *J. Appl. Electrochem.* **25** (1995) 450.
[12] F. C. Walsh, D. Pletcher, I. Whyte and J. P. Millington, *J. Chem. Tech. Biotech.* **55** (1992) 147.
[13] A. A. Wragg, *The Chemical Engineer* (*UK*), Jan. (1977) 39.
[14] J. R. Selman and C. W. Tobias, *Adv. Chem. Engng* **10** (1978) 211.
[15] D. A. Szánto and F. C. Walsh, unpublished work.
[16] E. J. Podlaha and J. M. Fenton, *J. Appl. Electrochem.* **25** (1995) 299.
[17] A. Montillet, J. Comiti and J. Legrand, *ibid.* **24** (1994) 384.
[18] D. Kyriacou, 'Modern Electroorganic Chemistry', Springer-Verlag, Berlin (1994).
[19] M. Darbarwar, V. Sundaramurthy and N. V. Subba, *Indian J. Chem.* **11** (1973) 115.
[20] C. J. Brown, D. A. Szanto, T. G. Nevell and F. C. Walsh, *J. Chem. Ed.*, submitted.
[21] I. Tabacovic, Z. Grujic and Z. Bejtovic, *J. Heterocyc. Chem.* **20** (1983) 635.
[22] M. A. Azzem, M. Zahran and E. Hagagg, *Bull. Chem. Soc. Japan* **67** (1994), 1390.
[23] P. Trinidad, D. Szánto and F. C. Walsh, 'Flow dispersion measurements in a laboratory filter-press cell', in preparation.